Zeitschrift: Schweizerische mineralogische und petrographische Mitteilungen = Bulletin suisse de minéralogie et pétrographie

Band: 85 (2005)

Heft: 1

Artikel: Zircon U-Pb geochronology and isotopic characterization for the pre-Mesozoic basement of the Northern Veporic Unit (Central Western Carpathians, Slovakia)

Autor: Gaab, A.S. / Poller, U. / Janák, M.

DOI: https://doi.org/10.5169/seals-1654

Schweizerische Mineralogische und Petrographische Mitteilungen 85, 69–88, 2005

Zircon U–Pb geochronology and isotopic characterization for the pre-Mesozoic basement of the Northern Veporic Unit (Central Western Carpathians, Slovakia)

A.S. Gaab [1], *U. Poller* [1], *M. Janák* [2], *M. Kohút* [3] and *W. Todt* [1]

Abstract

Ordovician magmatism can be observed in the whole Veporic unit. New single and multi-grain zircon U–Pb dating reveal an intensive magmatic activity between 470–460 Ma and a minor magmatic phase around 440 Ma in the Northern Veporic Unit. Carboniferous ages of SHRIMP and single grain TIMS U–Pb dating in this unit document intense metamorphism and magmatism during Variscan orogeny (350–330 Ma).

Previously published multi-grain U–Pb data in the same area have been interpreted to show Cambrian precursor ages. A new interpretation of this multi-grain data is suggested, revealing an Ordovician (464 ± 23) precursor age and a Carboniferous metamorphic overprint. Together with previously published data on the Southern Veporic Unit and the data presented in this study, a common Ordovician precursor age for the whole Veporic unit is recognized.

The isotopic signature for the Pre-Variscan basement in the Veporic unit is distinct from published data for the Tatric unit (Gneisses: $^{87}Sr/^{86}Sr_{ini,460}$ between 0.712 and 0.715; $\varepsilon Nd_{meas,460}$ between –8 and –10. Amphibolites: $^{87}Sr/^{86}Sr_{ini,460}$ between 0.708 and 0.710: $\varepsilon Nd_{ini,460}$ between 4.5 and 5.6). Only the Kralova Hola granites with a Variscan magmatic intrusion age between 330–360 Ma reveal distinct signatures and show similarities with diorites and granites from the High Tatra Mountains with $^{87}Sr/^{86}Sr_{ini,330}$ of 0.704 and 0.706 and $\varepsilon Nd_{ini,330}$ of –0.5 and –1.7.

Keywords: Ordovician, zircon, geochronology, isotope geochemistry.

1. Introduction

The pre-Variscan history of the Central Western Carpathians is not very well known. Late Cambrian to Ordovician protolith ages for meta-granitoids have been identified only recently in the poly-metamorphosed complexes of Veporic Unit (Putiš et al., 2001; Janák et al., 2002; Gaab et al., 2005). The Veporic Unit is one of three thick skinned north-verging Slovakocarpathian superunits (e.g. Plašienka et al., 1997). Its tectonic position is between the Tatric Unit in the North, which is dominated by Variscan magmatism (e.g. Poller and Todt, 2000), and the Gemeric Unit in the South, which is dominated by Palaeozoic sediments intruded by Permian granites (e.g. Vozárová et al., 1998; Poller et al., 2002).

Reliable radiometric ages on the Veporic Unit, especially U–Pb zircon ages for the pre-Variscan history, i.e. older than 360 Ma, are only sparsely available. U–Pb multi-grain dating by Putiš et al. (2001) reveals Cambrian protolith ages (514 ± 24 Ma) and Carboniferous ages (348 ± 31 Ma) in the poly-metamorphosed complexes of the northern region. ^{40}Ar–^{39}Ar step heating dating of an amphibolite revealed a staircase pattern with old apparent ages of up to 440 Ma indicating old cores in amphibole, which were partially reset by metamorphism (Maluski et al., 1993). Janák et al. (2002) presents chemical Th–U–Pb monazite dating with Ordovician (490–450 Ma) and Carboniferous ages (342 ± 27). Janák et al. (2002) interpreted this as a record of pre-Variscan granitoid magmatism and Variscan metamorphic overprint. Gaab et al. (2005), based on single zircon U–Pb dating, constrained an Ordovician age for the protolith (464 ± 40 Ma) and a Cretaceous age (82 ± 40) for the metamorphic overprint of the so called "Muráň Orthogneiss" in the southern part of the Veporic unit.

The U–Pb geochronological data imply significant differences in timing of pre-Variscan granitoid magmatism in the Veporic Unit. The purpose of this study is to resolve this age progression in

[1] Max-Planck-Institute for Chemistry, Section Geochemistry, P.O. Box 3060, D-55020 Mainz, Germany. <gaab@mpch-mainz.mpg.de>.<poller@mpch-mainz.mpg.ch>
[2] Slovak Academy of Sciences, Geological Institute, P.O. Box 106, 84005 Bratislava 45, Slovak Republic.
[3] Dionýz Stúr Institute of Geology, Mlynska Dolina 1, 81704 Bratislava, Slovakia.

0036-7699/05/0085/69

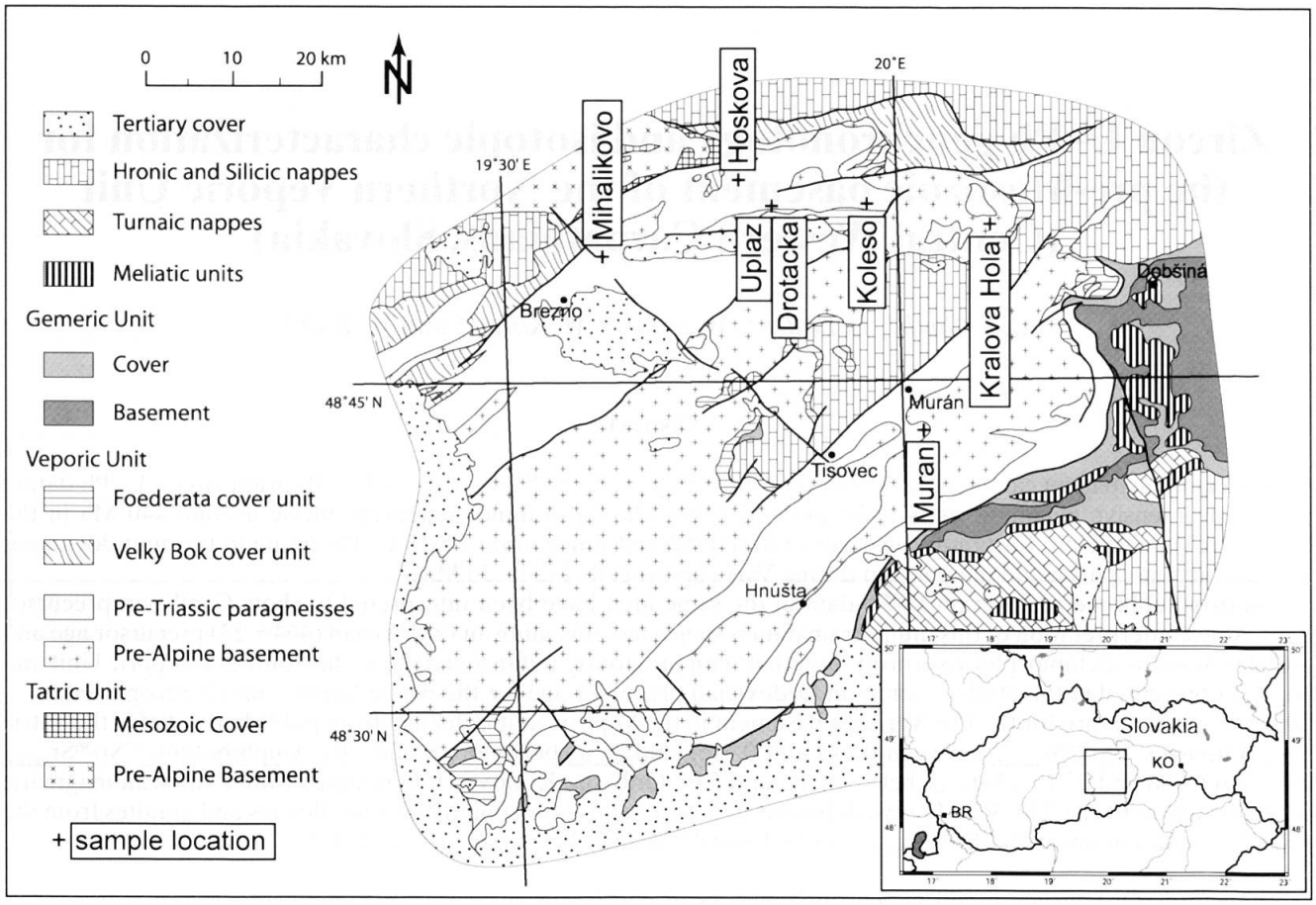

Fig. 1 Geological map of the Veporic Unit. Sample locations are indicated and location name used in this paper given. Outline of Slovakia with major rivers given in the inlay. Bratislava (BR) and Kosice (KO) are indicated.

detail by presenting zircon U–Pb dating from the basement rocks of the Northern Veporic Unit. The results together with a re-interpretation of the multi-grain data published by Putiš et al. (2001) argue against this dichotomy and a coeval evolution of the whole Veporic unit during Palaeozoic times is suggested by this study. In order to characterize the Northern Veporic Unit additional to the U–Pb zircon data, this study presents isotopic data for gneisses from the Koleso valley. This data are compared to the Tatric unit and to the southern part of the Veporic unit to resolve similarities and different source contributions.

2. Geological Setting

The Veporic Unit consist of pre-Alpine basement complexes assembled during the Variscan orogeny (Klinec, 1966; Zoubek, 1957; Andrusov, 1958) that are overlain by Upper Palaeozoic to Triassic sedimentary cover sequences (Fig. 1). The polymetamorphic basement comprises granitoids, migmatites, gneisses and amphibolites, mostly mylonitized during Alpine overprint. In the Central and North-Eastern part of the Veporic unit locally preserved para-autochthonous cover include Upper Permian sandstones and conglomerates, Scythian quarzites and slates, and Middle to Upper Triassic carbonates and shales (Foederata unit).

Variscan magmatic and metamorphic events in the Veporic basement have been determined by U–Pb dating of zircons in the granitoids, migmatites and orthogneisses (Cambel et al., 1990; Putiš et al., 2001). The Variscan age (370–330 Ma) of some Veporic granitoids has been documented also by chemical Th–U–Pb electron microprobe dating of monazite (Finger et al., 2003; Thöni et al., 2003). Some hornblende from basement amphibolites preserved pre-Alpine ages (377–346 Ma; Dallmeyer et al., 1996; Král' et al., 1996), however the ^{40}Ar–^{39}Ar do not show well defined plateau ages, suggesting metamorphic overprint. In the northern parts of the Veporic unit, in the Koleso valley, garnet-bearing metabasites bear evidence of eclogite facies metamorphism of unknown age (Janák et al., 2003). The host rocks of these eclogites show Variscan age of metamorphic recrystallization, based on Th–U–Pb chemical microprobe dating of monazite (Janák et al., 2002).

The grade of Alpine metamorphic overprint in the Northern Veporic Unit is not very well constrained, although at least greenschist to lower amphibolite facies conditions have been suggested for the basement (Putiš et al., 1997). Janák et al. (2001b) documented that Alpine overprint in the south-eastern parts of the Veporic basement reached middle amphibolite facies conditions (up to 620 °C and 10 kbar). All the Veporic cover units were affected by Alpine metamorphism of low to medium grade (Lupták et al., 2000, 2003). Published geochronological data provide Cretaceous metamorphic ages. The data include ^{40}Ar–^{39}Ar dating of micas and amphiboles (Maluski et al., 1993; Dallmeyer et al., 1996; Kováčik et al., 1996; Král' et al., 1996; Koroknai et al., 2001; Janák et al., 2001a) electron microprobe dating of metamorphic monazite (Janák et al., 2001b) and Sm–Nd dating of garnet (Lupták et al., 2004).

3. Analytical Techniques

Zircons were separated from crushed rocks using a Wilfley table, a Franz Magnetic Separator and Dijodmethane heavy liquid. Because of the CL control, no hand picking was necessary and the resin mounts were prepared from the unmagnetic (1.2 A), heavy fraction, which contained mainly zircons. The multi-grain fractions were sieved <74 μm in ethanol.

The SHRIMP (Sensitive High Resolution Ion Microprobe) analyses were performed at the ANU in Canberra. The standards SL13 and FC-1 were measured for reference after 3 spot analyses. Operating procedures for U, Th, and Pb isotopic measurements followed those described by Compston et al. (1984) and Williams (1998). For isotopic ratio calculation the SQUID program, version 1.02, was used (Ludwig, 2001b).

Isotope dilution U–Pb zircon analyses were performed at the MPI for Chemistry in Mainz. Inclusion free an simple grown zircons were selected according to their CL image for analysis. Digestion of the single zircon grains was performed in teflon bombs according to Wendt and Todt (1991) at 200 °C with HF–HNO_3 after addition of 3 μl ^{205}Pb–^{233}U mixed spike (corresponds to 80 pg ^{205}Pb and 17 ng ^{233}U) to each zircon. The multi-grain fractions were weighted and, after addition of ^{205}Pb–^{233}U mixed spike, digested with HF–HNO_3 in teflon bombs. Pb and U were separated using resin column chemistry (resin AG1-X8 100-200 mesh) after complete dissolution for the single as well as for the multi-grain analyses. The total Pb blank was generally less than 3 pg and was checked regularly during the analytics. The Pb and U fractions are loaded separately with silica gel on previously outgassed Re-single filaments. Their isotopic composition was measured on a Finnigan MAT 261 in dynamic mode equipped with an SEM operated in analog mode. All ratios were corrected for fractionation using the NBS 982 standard as reference (Todt et al., 1996). Common lead correction was applied using the Stacey and Kramers (1975) model composition at 460 Ma

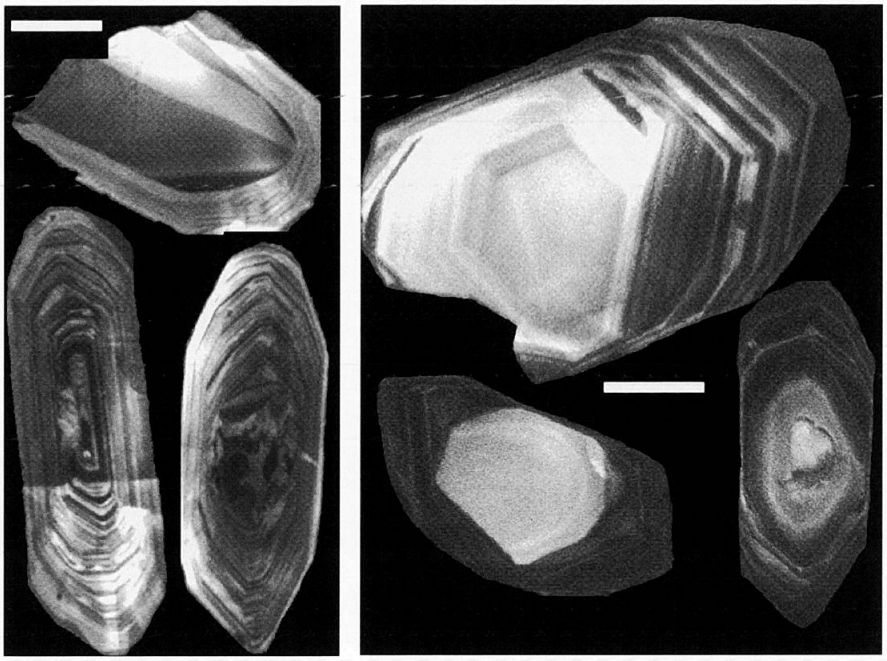

Fig. 2 Zircon CL images for the Kralova Hola samples 02GA14 (left) and 02GA17 (right). Scale bar indicates 50 μm.

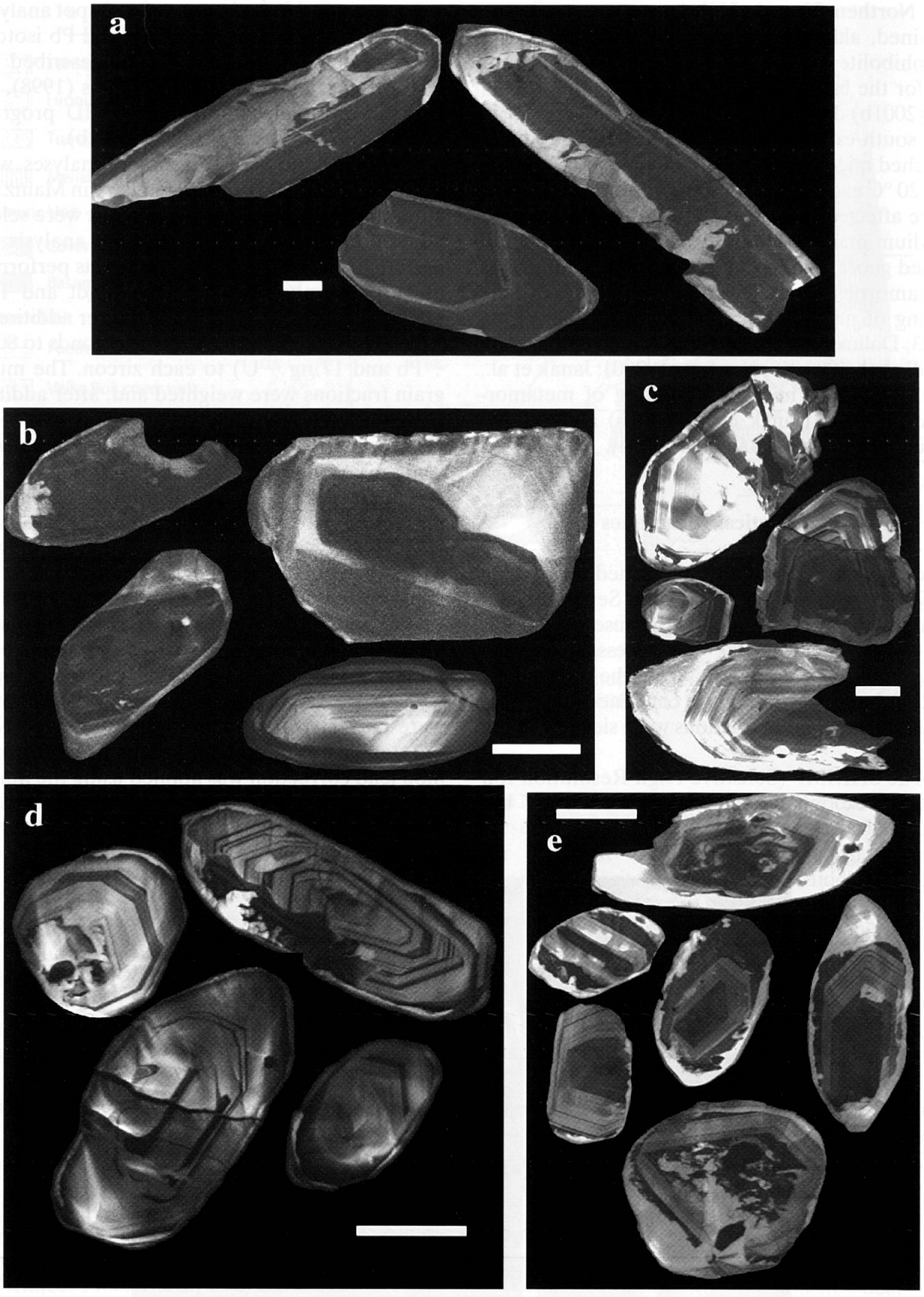

Fig. 3 Zircon CL images for samples from the Northern Veporic Unit. Localities shown in Fig. 1. Scale bar indicates 50 µm. Zircons were analysed by CL-controlled single grain vapor digestion technique (for sample 03GA50 also multi-grain conventional technique). Details on dating see Tables 2–4.
(a) Uplaz (03GA49). (b) Koleso (03GA18). (c) Mihalikovo (03GA50). (d) Drotacka (03GA48). (e) Hoškova (03GA61).

($^{206}Pb/^{204}Pb$: 17.99; $^{207}Pb/^{204}Pb$: 15.59; $^{208}Pb/^{204}Pb$: 37.80). Intentionally no individual common lead correction for the samples was performed to enhance the comparability between the samples. An individual common lead correction e.g. for the Koleso sample ($^{206}Pb/^{204}Pb$: 18.50; $^{207}Pb/^{204}Pb$: 15.65; $^{208}Pb/^{204}Pb$: 38.45) would yield in an 4–5 Ma younger age within error of the Stacey and Kramers (1975) correction, thus no significant offset is introduced by this.

CL images were obtained from resin mounts of the zircon separates. The resin was checked for Pb contamination by blank measurements using the TIMS and no significant amount of Pb was detected. The mounts were polished using diamond polishing suspensions. CL and BSE images were obtained by the scanning electron microscope Hitachi S450 with 15 kV accelerating voltage equipped with a CL-detector.

Main and trace elements were analyzed on powder and melt tablets by RFA at the University of Mainz. For Sr and Nd isotopic analyses the powdered whole rock samples were dissolved using a microwave assisted acid digestion as described in Gaab et al. (2005) and were separated using column chemistry according to White and Patchett (1984). For WR-Pb–Pb analyses rock splits were leached in HF–HNO_3 and Pb was separated using resin column chemistry as described in Gaab et al. (2006). The isotopic data for Pb, Sr and Nd was measured at the MPI for Chemistry in Mainz using a Finnigan MAT261 in static mode.

4. Samples for Geochronology

Samples for single and multi-grain U-Pb zircon studies were taken on the southern slope of the mountain ridge "Král'ovohol'ske Tatry" north of the village Helpa in Central Slovakia. Additional the Hoškova sample was taken along the northern slope of this mountain ridge according to the outcrop described in Putiš et al. (2001). The location names were assigned according to the topographic map "Turistická mapa 1:50 000 'Nízke Tatry Král'ova Hol'a' no.123, 3.vydanie".

The samples from Kralova Hola were analyzed by SHRIMP, the other samples were analyzed by the vapor digestion single grain or conventional mulit-grain technique.

4.1. Kralova Hola

Kralova Hola is the easternmost peak along the Král'ovohol'ske Tatry mountain ridge. Sample 02GA14 was taken near the top at 48° 52' 20"N; 20° 09' 20"E. It is a strongly mylonitized granitic feldspar-augen gneiss. Additional an undeformed granite (Sample 02GA17) was sampled at 48° 50' 40"N; 20° 07' 52"E. Petrographically and geochemically these two samples are very similar, only the degree of tectonic deformation is diffferent. Zircon CL images for both samples are shown in Fig. 2. In general, the zircons are simple euhedral magmatic zircons with magmatic zoning as seen by oscillatory magmatic growth in Fig. 2. No metamorphic rim can be observed. Only a minor part of the zircons exhibit small remnants of cores.

4.2. Koleso valley

For the U–Pb zircon dating sample 03GA18, a granitoid boudin in strongly deformed felsic gneisses was sampled at 48° 53' 55"N; 19° 59' 15"E.

The zircons of this sample (Fig. 3b) have a low CL brightness. They show magmatic zoning in the central parts. The rims are strongly influenced by resorption and recrystallization effects, thus the zircons appear quite rounded in the CL image (Fig. 3b).

4.3. Uplaz and Drotacka

Samples for U–Pb single zircon analyses were taken at 48° 52' 50"N; 19° 54' 50"E on the southern slope of the Král'ovohol'ske mountain ridge 3.5 km north of Závadka nad Hronom.

In the Uplaz valley sample 03GA49 was taken along a roadside cliff. This sample resembles an intermediate to felsic gneiss, strongly deformed and quite similar to the felsic gneisses in the Koleso valley. CL zircon images are shown in Fig. 3a and reflect intense resorption and recrystallization features at the rims. Magmatic zoning is present in the inner parts of the zircons, which reveal a low CL brightness.

Sample 03GA48 resembles a fine-grained granitoid with no apparent deformation, very untypical for the basement in this area. It was sampled on the Drotacka ridge, 500 m east of sample 03GA49. CL zircon images are show in Fig. 3d. The zircons show intensive magmatic zoning. Nevertheless resorption structures can be observed in most grains.

4.4. Mihalikovo quarry

Directly above the abandoned quarry near the Mihalikovo valley at 48° 50' 05"N; 19° 39' 35"E sample 03GA50 was taken at a small cliff consisting of strongly layered and deformed intermediate gneisses. The CL images of the zircons from

this sample are shown in Fig. 3c. The inner parts of these zircons show magmatic zoning, but the zircons also exhibit intensive resorption and metamorphic rims.

4.5. Hoškova valley

The sample 03GA61 is taken near to the outcrop described for the sample VBNT-76L in Putiš et al. (2001) at 48° 55 '22"N; 19° 53 '55"E. The sampled cliff is 50 m above the road opposite to the small creek on the southern slope of the ridge. The cliff consists of strongly banded amphibolites interlayered with Pl–Qtz rich felsic gneisses.

Zircons for this felsic gneiss are presented in Fig. 3e. They show magmatic zoning in the inner parts but also strong resorption structures and rims with a bright CL intensity most probable linked to a metamorphic overprint.

5. Samples for Geochemistry

Samples for the geochemical studies were sampled in the Koleso valley north-east from Helpa and on top of Kralova Hola (Fig. 1).

5.1. Koleso Valley

In the Koleso valley a large variety of basement rocks occur. Most prominent are felsic gneisses with variable amount of SiO_2 present (Table 5).

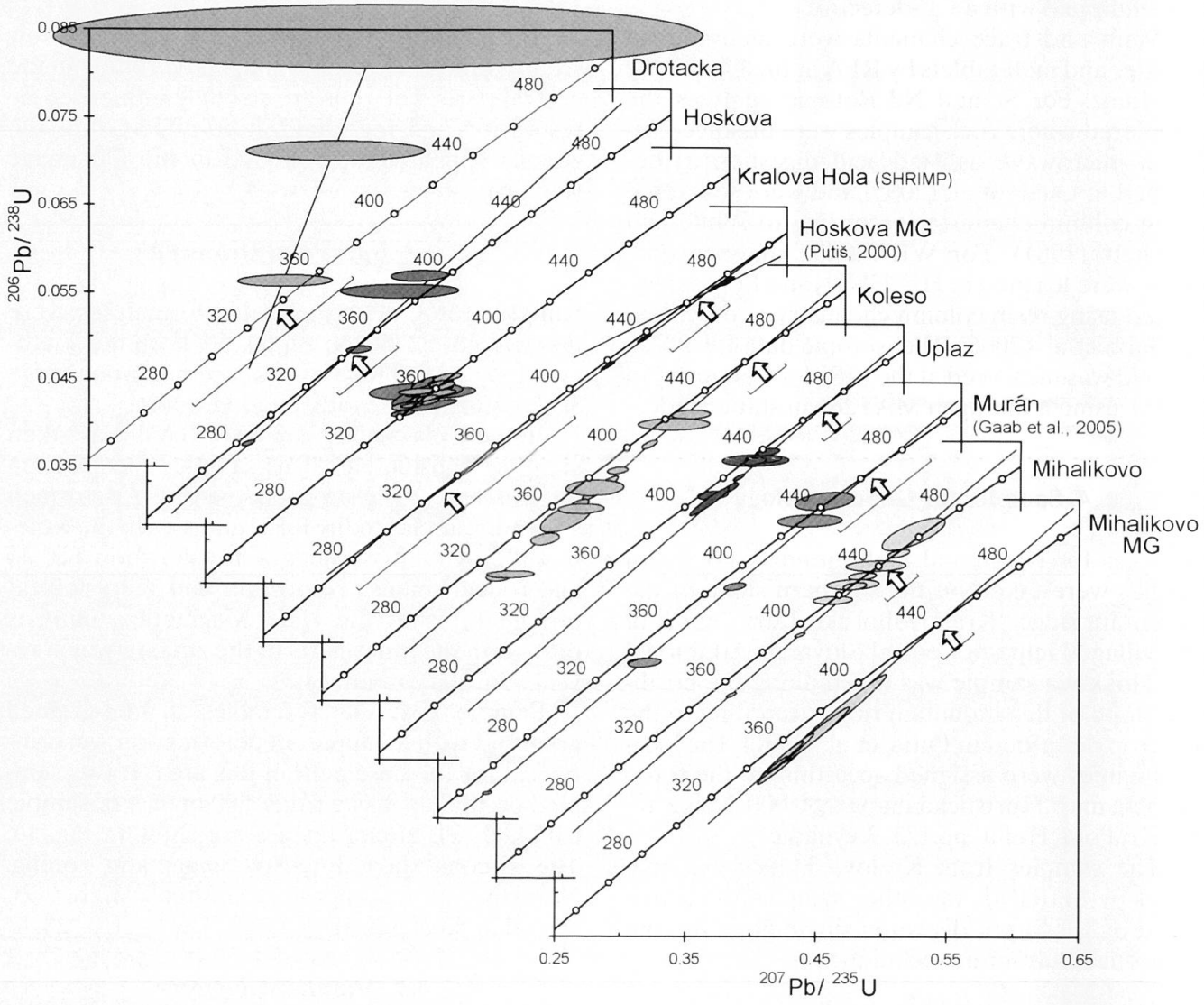

Fig. 4 Compilation of the U–Pb zircon data to identify the two main magmatic/metamorphic events recorded in the Veporic basement. Intercept ages and error bars are indicated by the arrows. Please note that the x- and y- axis are shifted for each sample. Data from Gaab et al. (2005) and from Putiš et al. (2001) given for comparison. Please note that the discordia lines for the latter dataset differ from the originally published one. For detailed argumentation see chapter 6.3. The Kralova Hola data are measured on SHRIMP (Table 1), all other data are TIMS measurements (Table 2). Lower intercept ages are recent except for the Muráň (Gaab et al., 2005) sample (see Table 4).

Intercalated with these felsic gneisses are garnet-bearing amphibolites. All samples show intense deformation and exhibit lineations.

For geochemical analyses samples for the felsic gneisses (02GA01, 02GA06 and 02GA10) and for the amphibolites (02GA04, 02GA11 and 02GA12) were collected in this valley. In addition, a gabbro with magmatic features, sample 02GA 08, was sampled for comparison with the amphibolites. To record the Pb isotopic variation of these rocks, samples 02GA01–02GA12 and samples 03GA25–03GA32, taken from the same outcrop as sample 03GA18, were used for WR-Pb–Pb analyses.

5.2 Kralova Hola

The samples used for geochronology (02GA14 and 02GA17) were also analyzed for their isotopic composition.

6. U–Pb zircon dating results

U–Pb zircon dating presented in this study was performed on 7 samples from the Northern Veporic Unit. Locations of these samples are indicated in Fig. 1 and zircon CL images of each sample are show in Fig. 2 to Fig. 3c. The data for the individual grains are given in Table 1 for the SHRIMP analyses and in Table 2 for the single grain and mulit-grain analyses. The concordia diagrams are presented in Fig. 4 as a compilation of all samples to pronounce similarities and differences observed for the samples. Table 4 presents the exact upper and lower intercept ages for all samples investigated in this study. Discordia ages and diagrams were generated using ISOPLOT (Ludwig, 2001a).

6.1. SHRIMP dating

The samples from Kralova Hola (02GA14 and 02GA17) were dated by SHRIMP. Both samples belong to the same lithological unit, which is demonstrated by similar isotopic composition of these samples (Table 5). Also the zircon populations of both samples are very similar (Fig. 2).

The measurements for both samples does not result in a concordant age, even if the individual measurements are mostly concordant for themselves (Table 1). That the populations are not concordant is most probably generated by an underestimation of the analytical error of the individual measurements. Nevertheless a good overlap for both samples can be observed in the concordia diagram (Fig. 4). The mean $^{206}Pb/^{238}U$ age results in an age of 356 ± 10 and 359 ± 6 (02GA14 and 02GA17, respectively), which overlap within error with the discordia ages of 349 ± 26 and 345 ± 11, when calculating with recent lead loss (Table 1 and Table 4). This age of ≈ 350 Ma is, in accordance with the CL images (Fig. 2), interpreted as magmatic intrusion age.

Cores are present to a minor extend in zircons of both samples and reveal $^{207}Pb/^{206}Pb$ ages between 1700 and 1500 Ma.

6.2. Conventional dating

The Koleso and the Uplaz samples reveal similar upper intercept ages of 462 ± 10 and 467 ± 8 Ma, respectively (Table 4). Individual grains are discordant and a discordia line with a lower intercept at recent times can be inferred (Fig. 4). $^{206}Pb/^{204}Pb$ ratios are between 80 and 900 for the Koleso sample and between 65 and 2650 for the Uplaz sample (Table 2). One zircon of the Koleso sample reveals an old $^{207}Pb/^{206}Pb$ age of 1500 Ma. Two grains of this sample reveal slightly older ages as the upper intercept age of the discordia (Table 2) and they are not used for regression (Fig. 4). Nevertheless plot these grains in agreement with the discordia line intersecting the concordia at 462 Ma and recent times. These ages are interpreted as magmatic intrusion ages, as the CL images of the zircons show clearly magmatic oscillation in the cores (Fig. 3b and Fig. 3a).

A slightly younger intrusion age of 440 ± 7 is revealed by the single grain data of the Mihalikovo sample. This age is additionally constrained by multi-grain data on the zircon sieve fraction <74 μm. The multi-grain measurements, with $^{206}Pb/^{204}Pb$ ratios between 2860 and 4450, result in an upper intercept age of 443 ± 6 and recent lead loss (Table 2 and 4). Details of the multi-grain measurements are given in Table 3.

The ratio of the radiogenic lead (Pb*) and the weight of zircon fraction records the effect of the HNO_3 wash step. Washed fractions have ratios of ≈ 50, whereas the not washed fractions have lower ratios between 32 and 43 (Table 3). This documents that during washing a large amount of less radiogenic minerals were dissolved resulting in an increase of the radiogenic lead measured. Nevertheless, this does not influence the results of the multi-grain dating, because all fractions plot nicely along one discordia line. The single grain data of this sample plot closer to the concordia line than the multi-grain data. The zircons used for single grain dating were mostly larger than 100 μm (Fig. 3c), whereas for the multi-grain dating only zircons smaller than 74 μm were used. Therefore a correlation between the discordancy and

Table 1 Data for the SHRIMP analyses of the Kralova Hola. Concordia diagram shown in Fig. 4

zircon grain no.	location name	measured ratios $^{204}Pb/^{206}Pb$	$^{207}Pb/^{206}Pb$	% err	$^{208}Pb/^{206}Pb$	% err	% discordant	% ^{206}Pb comm	ppm U	ppm Th	$^{232}Th/^{238}U$	^{204}Pb corrected $^{206}Pb/^{238}U$	1σ	$^{207}Pb/^{235}U$	1σ	cor.	calculated ages $^{206}Pb/^{238}U$	1σ	$^{207}Pb/^{206}Pb$	1σ
2.1	Kralova Hola	9.7E-5	.0544	0.8	.220	0.9	-9	0.18	801	544	0.70	0.0580	0.0003	0.427	0.006	0.68	356.9	3.8	399	43
2.2	02GA14	2.5E-4	.0559	0.8	.197	1.0	-14	0.45	802	468	0.60	0.0555	0.0002	0.405	0.007	0.50	362.2	3.8	349	26
3.1	-"-	1.6E-4	.0546	1.0	.167	1.4	-15	0.29	468	244	0.54	0.0554	0.0004	0.400	0.008	0.47	353.8	3.7	386	23
9.1	-"-	8.9E-5	.0546	0.9	.212	1.1	-3	0.16	630	405	0.67	0.0563	0.0003	0.417	0.007	0.62	361.4	3.9	328	27
9.2	-"-	6.1E-5	.0539	0.7	.185	0.9	-8	0.11	877	509	0.60	0.0569	0.0003	0.418	0.005	0.76	348.9	3.6	299	41
11.1	-"-	1.5E-4	.0569	1.1	.164	1.5	12	0.27	440	214	0.50	0.0569	0.0003	0.428	0.010	0.49	348.9	3.7	298	46
17.1	-"-	7.1E-5	.0545	0.8	.173	1.0	-4	0.13	870	463	0.55	0.0572	0.0003	0.421	0.006	0.68	350.9	3.6	341	31
18.1	-"-	1.9E-5	.0546	0.9	.212	1.1	9	0.03	544	362	0.69	0.0559	0.0003	0.420	0.006	0.73	355.8	3.6	328	20
23.1	-"-	5.0E-4	.0612	0.7	.205	1.0	4	0.90	733	436	0.61	0.0569	0.0003	0.422	0.009	0.37	354.0	3.7	368	60
24.1	-"-	8.4E-5	.0547	1.2	.136	1.7	-5	0.15	338	137	0.42	0.0587	0.0004	0.433	0.009	0.57	367.4	4.0	348	36
32.1	-"-	7.5E-5	.0555	0.9	.186	1.3	7	0.14	590	334	0.58	0.0577	0.0004	0.431	0.007	0.66	362.4	3.8	389	27
41.1	-"-	1.5E-4	.0542	0.8	.136	1.2	-21	0.28	790	329	0.43	0.0570	0.0004	0.409	0.007	0.55	358.8	3.7	284	37
45.1	-"-	6.0E-5	.0533	1.0	.212	1.0	-14	0.11	652	431	0.68	0.0569	0.0003	0.413	0.006	0.62	354.9	3.7	304	31
48.1	-"-	5.3E-5	.0543	0.9	.238	1.1	-5	0.10	696	492	0.73	0.0582	0.0003	0.429	0.008	0.67	367.7	3.8	349	27
50.1	-"-	2.3E-5	.0533	0.6	.010	3.0	-8	0.04	1506	46	0.03	0.0585	0.0003	0.428	0.004	0.86	362.5	3.7	325	14
50.2	-"-	2.5E-5	.0533	0.6	.199	0.9	-10	0.05	1347	836	0.64	0.0563	0.0003	0.410	0.005	0.81	354.2	3.6	326	17
52.1	-"-	---	.0542	0.7	.162	1.1	4	0.01	1106	548	0.51	0.0580	0.0003	0.432	0.004	0.85	364.1	3.7	379	15
53.1	-"-	2.0E-4	.0554	1.1	.206	1.3	-15	0.36	412	255	0.64	0.0571	0.0003	0.410	0.012	0.38	360.3	3.9	306	60
60.1	-"-	1.6E-5	.0537	0.9	.218	1.1	-5	0.03	602	397	0.68	0.0583	0.0004	0.427	0.006	0.66	366.4	3.8	348	27
68.2	-"-	4.9E-5	.0543	0.7	.138	1.1	-4	0.09	992	419	0.44	0.0583	0.0002	0.431	0.004	0.76	365.8	3.7	352	20
																mean age	**358.9**	**6.0**	**340.3**	**33**
68.1	-"-	3.7E-5	.1037	0.5	.184	0.8	17	0.06	314	173	0.57	0.2546	0.0019	3.634	0.039	0.88	1436.6	13.8	1682	10
17.1	Kralova Hola	1.5E-4	.0540	1.1	.046	2.9	-23	0.27	409	58	0.15	0.0581	0.0006	0.416	0.009	0.80	362.0	4.8	279	37
22.1	02GA17	1.4E-4	.0564	1.7	.177	2.3	10	0.27	193	107	0.57	0.0555	0.0005	0.422	0.015	0.80	350.5	4.1	387	57
22.2	-"-	3.8E-5	.0541	0.5	.030	1.6	-4	0.07	2176	206	0.10	0.0573	0.0003	0.424	0.003	0.80	366.8	3.7	353	14
27.1	-"-	7.4E-5	.0549	1.1	.106	1.7	1	0.13	587	199	0.35	0.0573	0.0004	0.428	0.008	0.80	359.7	4.0	363	32
29.1	-"-	4.7E-4	.0571	2.3	.145	3.4	-43	0.86	87	37	0.44	0.0571	0.0008	0.409	0.029	0.26	359.2	5.6	206	135
29.2	-"-	2.1E-4	.0571	0.5	.029	1.8	10	0.38	1878	100	0.05	0.0563	0.0007	0.400	0.008	0.80	338.3	3.4	371	28
41.1	-"-	6.1E-5	.0547	1.1	.041	2.8	0	0.11	411	48	0.12	0.0573	0.0004	0.420	0.009	0.58	360.6	3.8	361	34
41.2	-"-	8.2E-5	.0539	1.0	.038	2.9	-8	0.15	458	49	0.11	0.0575	0.0003	0.429	0.005	0.81	341.2	3.6	314	40
44.1	-"-	1.6E-5	.0544	0.7	.229	1.3	5	0.03	1431	995	0.72	0.1281	0.0010	1.667	0.020	0.90	359.7	4.0	377	18
47.1	-"-	2.6E-4	.0587	1.8	.228	2.2	14	0.47	140	95	0.70	0.0569	0.0005	0.431	0.020	0.32	358.2	4.4	410	82
																mean age	**355.6**	**9.3**	**342.2**	**60**
44.2	-"-	6.7E-5	.0946	0.6	.100	1.4	92	0.11	355	73	0.21	0.0546	0.0003	0.398	0.007	0.52	783.1	10.3	1501	13

Table 2 Data for the U–Pb zircon analyses shown in Fig. 4. MG – multi-grain; SG – single grain; CLC – single grain with CL control. Analyses used for calculation of the discordias are indicated.

sample name	location name	type	Pb* (ng)	Pb_{comm} (ng)	U_{tot}/Pb_{rad}	$^{206}Pb/^{204}Pb$	2σ	corrected ratios $^{207}Pb/^{206}Pb$	2σ	$^{208}Pb/^{206}Pb$	2σ	calculated ages $^{206}Pb/^{238}U$	2σ	$^{207}Pb/^{235}U$	2σ	$^{207}Pb/^{206}Pb$	2σ	used for discordia
K62	Drotacka	CLC	0.013	0.013	11.2	71	1.6	0.2476	0.0063	0.5436	0.0166	522	18	391	152	--	--	*
K30	"	CLC	0.025	0.022	13.1	85	1.2	0.2169	0.0013	0.4699	0.0020	443	6	368	40	--	--	*
K66	"	CLC	0.054	0.010	16.1	281	14.1	0.1024	0.0004	0.1907	0.0014	353	3	340	22	249	162	*
K18	Hoskova	CLC	0.004	0.007	17.5	45	0.6	0.3521	0.0015	0.8113	0.0052	360	11	149	92	--	--	
L107	"	CLC	0.039	0.078	18.8	48	0.6	0.3520	0.0014	0.8431	0.0027	294	15	274	69	--	--	
L151	"	CLC	0.004	0.002	15.6	62	1.4	0.2586	0.0009	0.5794	0.0051	395	8	208	90	--	--	
L17	"	CLC	0.007	0.004	12.2	82	0.7	0.2066	0.0012	0.4564	0.0029	492	8	279	40	--	--	
L125	"	CLC	0.021	0.003	13.2	217	2.4	0.1138	0.0006	0.2324	0.0015	425	3	382	13	128	77	
K59	"	CLC	0.034	0.016	13.9	129	1.1	0.1645	0.0003	0.3668	0.0010	398	3	382	13	285	82	*
K29	"	CLC	0.045	0.008	14.7	275	12.2	0.1037	0.0010	0.1845	0.0017	387	4	371	27	272	193	*
L28	"	CLC	0.103	0.009	16.2	542	7.6	0.0802	0.0002	0.1364	0.0011	346	2	348	6	363	34	*
K43	"	CLC	0.344	0.018	20.3	1062	3.0	0.0666	0.0003	0.0987	0.0008	280	2	286	3	329	17	*
L17	Mihalikovo	MG	121.160	2.702	15.9	2864	8.7	0.0607	0.0001	0.0945	0.0002	349	8	361	8	437	12	*
M1	"	MG	280.442	5.719	14.8	3166	6.8	0.0607	0.0001	0.0815	0.0002	378	23	389	21	457	24	*
L39	"	MG	156.576	3.125	16.2	3197	9.4	0.0603	0.0001	0.0939	0.0002	343	5	356	5	441	7	*
M3	"	MG	238.672	4.414	15.4	3222	6.7	0.0607	0.0001	0.0822	0.0002	364	16	377	15	458	19	*
M2	"	MG	324.799	6.397	16.3	3250	6.7	0.0607	0.0001	0.0905	0.0002	343	11	358	11	459	14	*
L2	"	MG	129.719	2.504	15.9	3299	9.6	0.0601	0.0001	0.0945	0.0002	349	13	362	12	440	15	*
L42	"	MG	90.165	1.290	16.4	4445	10.8	0.0590	0.0001	0.0897	0.0002	340	6	353	6	439	6	*
L50	Mihalikovo	CLC	0.290	0.407	15.6	62	0.2	0.2882	0.0005	0.6696	0.0018	354	4	352	13	341	216	
L76	"	CLC	0.050	0.020	14.0	155	11.1	0.1472	0.0005	0.2318	0.0033	392	6	389	57	374	374	
K61	"	CLC	0.055	0.016	14.9	195	17.0	0.1233	0.0003	0.2771	0.0010	369	5	340	51	142	344	
K112	"	SG	0.186	0.042	12.5	277	4.5	0.1078	0.0006	0.2153	0.0022	440	3	439	13	430	79	*
K98	"	SG	0.156	0.026	11.8	349	4.4	0.0970	0.0002	0.1941	0.0006	462	9	457	13	434	41	*
L148	"	CLC	0.147	0.013	12.5	578	9.7	0.0801	0.0002	0.1623	0.0005	433	2	432	6	423	29	*
K101	"	CLC	0.121	0.009	12.8	621	8.4	0.0786	0.0001	0.1574	0.0008	426	2	428	5	437	22	*
L159	"	CLC	0.290	0.026	13.2	633	23.3	0.0780	0.0002	0.1490	0.0007	416	2	416	8	416	48	*
L8	"	SG	0.684	0.061	20.7	706	3.9	0.0742	0.0001	0.1152	0.0005	275	2	284	3	354	23	
K45	"	SG	0.468	0.025	13.7	1005	6.2	0.0701	0.0001	0.1496	0.0002	392	1	399	2	441	8	*
K45	"	CLC	0.270	0.013	12.9	1099	92.1	0.0684	0.0002	0.1145	0.0010	427	3	427	11	424	57	*
K28	"	CLC	0.310	0.012	12.2	1321	31.2	0.0669	0.0001	0.1202	0.0005	449	2	450	5	456	17	*
K24	"	SG	1.408	0.045	16.0	1870	20.1	0.0634	0.0001	0.0932	0.0002	351	2	362	2	439	8	*

Table 2 (continued). MG – multi-grain; SG – single grain; CLC – single grain with CL control. Analyses used for calculation of the discordias are indicated.

sample	location	name	type	Pb* (ng)	Pb_{comm} (ng)	U_{tot}/Pb_{rad}	$^{206}Pb/^{204}Pb$	2σ	corrected ratios $^{207}Pb/^{206}Pb$	2σ	$^{208}Pb/^{206}Pb$	2σ	calculated ages $^{206}Pb/^{238}U$	2σ	$^{207}Pb/^{235}U$	2σ	$^{207}Pb/^{206}Pb$	2σ	used for discordia
A52-5	Koleso	SG		0.943	0.954	16.4	84	0.3	0.2292	0.0004	0.4605	0.0011	358	3	375	10	479	120	*
A25-2	"	SG		1.828	1.592	15.8	96	0.6	0.2081	0.0004	0.4048	0.0010	373	4	382	13	440	170	*
A55-4	"	SG		0.329	0.232	14.1	112	1.0	0.1859	0.0005	0.3453	0.0010	417	3	424	15	465	117	*
A55-1	"	SG		1.518	0.796	13.9	147	0.5	0.1556	0.0005	0.2647	0.0007	423	3	433	8	483	66	*
A25-5	"	SG		0.890	0.451	19.0	151	1.8	0.1538	0.0004	0.2593	0.0012	312	2	336	11	502	97	*
A52-7	"	SG		0.261	0.245	19.2	155	0.7	0.1502	0.0002	0.2509	0.0006	310	2	329	6	464	62	*
A52-1	"	SG		1.883	0.889	16.9	161	0.9	0.1447	0.0002	0.2419	0.0008	352	8	367	12	463	61	*
A52-2	"	SG		1.888	0.851	16.7	168	0.8	0.1426	0.0002	0.2312	0.0006	356	3	370	6	453	57	*
A55-2	"	SG		5.960	2.592	17.6	174	0.7	0.1502	0.0002	0.2236	0.0006	337	3	355	7	473	51	*
A25-3	"	SG		1.122	0.372	19.2	222	0.9	0.1222	0.0003	0.1748	0.0006	311	2	331	5	472	40	*
A25-1	"	SG		0.315	0.068	15.4	319	2.2	0.1016	0.0001	0.1239	0.0005	385	2	395	5	452	30	*
A52-3	"	SG		2.636	0.473	16.0	395	1.8	0.0931	0.0001	0.0989	0.0003	373	7	385	8	461	20	*
A52-6	"	SG		2.818	0.448	16.5	444	2.3	0.0888	0.0001	0.0883	0.0003	361	3	374	5	452	21	*
A25-4	"	SG		3.319	0.259	14.8	881	4.7	0.0728	0.0001	0.0455	0.0001	403	2	412	3	463	14	*
A55-5	"	SG		0.346	0.037	9.6	579	12.7	0.0821	0.0003	0.0982	0.0005	595	5	575	11	495	39	
A55-3	"	SG		0.182	0.016	11.6	709	20.6	0.0777	0.0003	0.1059	0.0004	485	3	489	10	507	43	
A52-4	"	SG		2.078	0.223	6.0	574	5.8	0.1185	0.0002	0.1622	0.0004	849	4	1057	6	1515	13	old core
K30	Uplaz	CLC		0.290	0.381	12.9	67	0.2	0.2742	0.0006	0.6138	0.0019	432	3	436	14	459	137	*
K64	"	CLC		0.710	0.293	12.7	170	1.2	0.1422	0.0002	0.2943	0.0007	433	2	440	8	478	55	*
K46	"	CLC		1.940	0.285	13.2	434	7.5	0.0895	0.0001	0.1954	0.0005	408	2	414	7	449	38	*
K60	"	CLC		4.360	0.332	13.1	825	3.4	0.0743	0.0001	0.1515	0.0004	413	3	423	4	480	11	*
L108	"	CLC		0.410	0.021	12.4	1072	19.5	0.0698	0.0002	0.1299	0.0005	438	2	442	5	465	21	*
K62	"	CLC		5.177	0.272	13.6	1202	18.4	0.0683	0.0001	0.1213	0.0003	404	8	412	9	461	14	*
L122	"	CLC		0.406	0.017	12.6	1229	27.8	0.0679	0.0002	0.1263	0.0003	432	2	436	5	460	20	*
L102	"	CLC		1.156	0.025	13.1	2617	21.0	0.0619	0.0001	0.0980	0.0003	421	2	428	3	467	7	*

the grain size becomes apparent. Smaller zircons display a larger degree of discordancy (Fig. 4).

The CL images of the zircons show recrystallization and resorption effect at the rims, nevertheless are the upper intercept ages interpreted as magmatic intrusion ages, as the inner parts clearly show magmatic oscillatory zoning (Fig. 3c).

Younger ages are revealed by the Hoškova and the Drotacka samples. Most analyses of these samples resulted in $^{206}Pb/^{204}Pb$ ratios below 100 and were discarded. Nevertheless, some analyses gave reasonable ratios and result in upper intercept ages of 334 ± 19 and 329+72–34, respectively (Fig. 4, Table 4). As can be seen in Table 2, the U concentrations in the zircons are very low and therefore accordingly also the radiogenic lead concentrations. This results in a large common lead correction and some analyses are not used for regression (indicated also in Table 2). The reverse discordancy of some analyses is produced by the analytical uncertainty and therefore mainly in the common Pb correction. Nevertheless, the low $^{206}Pb/^{204}Pb$ ratios were reproducible for separate dissolution steps for both samples. Thus this is not due to contamination, but due to low U and therefore the low radiogenic lead concentrations of the zircons.

6.3 Discussion of the U–Pb data

The compilation of all U–Pb zircon data is presented in Fig. 4 and in Table 4. Additional to the samples presented in this study the single grain data presented in Gaab et al. (2005, Muráň gneiss, locality indicated in Fig. 1) and the multi-grain data for the sample VBNT-76L published in Putiš et al. (2001, sample from the Hoškova locality indicated in Fig. 1) are included. Please note that the latter data are reinterpreted and the intercept ages do not correspond to the originally published. This will be discussed in more detail below.

A good accordance in the upper intercept can be observed for Koleso (03GA18), Uplaz (03GA49) and Muráň sample (UP1115) (Gaab et al., 2005). All these have an upper intercept age between 470 and 460 Ma. Most zircon analyses of these samples are discordant, but

Table 3 Details of multi-grain analyses of sample 03GA50(MG) from Mihalikovo. Pb* and results given in Table 2.

analysis no.	sieve fraction [μm]	weight of fraction [mg]	weight of spike [mg]	HNO3 wash	Pb* / weight of fraction
M1	<74	8.778	.015	no	32
M2	<74	7.559	.015	no	43
M3	<74	6.029	.015	no	39
L39	<74	3.077	.019	yes	51
L2	<74	2.615	.019	yes	49
L17	<74	2.405	.016	yes	50
L42	<74	1.815	.012	yes	49

only the Muráň sample reflects a clear Alpine lower intercept age of 88 ± 40 Ma (Gaab et al., 2005). The two other samples are interpreted to show recent lead loss (see Table 2). Recently described HP-metamorphism in the area of the Koleso valley (Janák et al., 2003) is not recorded in the U–Pb systematics of the zircon. If this is due to sampling or if the HP event did not influence the U–Pb systematics of the zircons in the Koleso valley can not be discussed with the available data. Only the zircons of the Muráň area record a Cretaceous event, where intensive and pervasive metamorphism is described (Janák et al., 2001a; Lupták et al., 2000).

The Mihalikovo sample (03GA50) yields a slightly younger upper intercept age of ≈ 440 Ma for both, the single grain analyses and the multigrain analyses. Two single zircons yield $^{206}Pb/^{238}U$ ages older than 440 Ma (449 ± 2 Ma and 462 ± 9 Ma) indicating slightly older components present in the zircons. Recent lead loss must be assumed for this sample.

A completely different age spectrum is given by the Drotacka (03GA48) and Hoškova sample (03GA61). Zircons of both samples have extremely low uranium and radiogenic lead contents. Nevertheless both samples yield discordia intercept ages between 360 and 320 Ma, which are clearly distinct from the ages of the previously described samples. Similar Variscan ages are also observed for the Kralova Hola samples (02GA14 and 02GA17) by SHRIMP dating presented in this work.

The Ordovician ages of the Uplaz, Koleso and Mihalikovo samples are interpreted as magmatic formation ages in concordance with the CL-images. The ages for the Kralova Hola samples clearly indicate a Variscan magmatic event (see Fig. 2), even if the sample 02GA14 is strongly mylonitized. The nearly identical ages for the deformed and the undeformed sample proof that this deformation and metamorphism did not influence the U–Pb system of the zircons. Also the ages of the Drotacka sample are interpreted as magmatic ages, because of the apparent absence of deformation of the specimen and of the mainly magmatic zoning present in the CL images. Only for the Hoškova sample it must be discussed, if the

Table 4 Compilation of the intercept ages shown in Fig. 4. Reinterpreted data from Putiš et al. (2001) and the data from Gaab et al. (2005) are included.

Sample Name	Location name	lower intercept	+2σ	-2σ	upper intercept	+2σ	–2σ	no. of points	MSWD	Probability of fit
03GA48	Drotacka	-	-	-	329	34	72	3	0	0.99
03GA61	Hoškova	0	0	0	334	19	19	4	1.2	0.31
02GA14	Kralova Hola	0	0	0	345	11	11	20	1.1	0.34
02GA17	Kralova Hola	0	0	0	349	26	26	11	2.3	0.02
VBNT-764a[1]	Hoškova	464	8.3	23	1297	1100	790	2	0	1
VBNT-764b[1]	Hoškova	333	120	110	489	77	50	2	0	1
03GA18	Koleso	0	0	0	461.6	9.8	9.9	14	0.3	0.99
03GA49	Uplaz	0	0	0	468.6	7.8	7.9	8	0.76	0.62
UP1115 2	Muran	88	34	40	464	36	33	6	0.36	0.84
03GA50SG	Mihalikovo	0	0	0	439.8	6.6	6.6	9	0.47	0.88
03GA50MG	Mihalikovo	0	0	0	442.6	6.1	6.2	7	1.7	0.12

[1] reinterpreted intercepts of multigrain data from Putiš et al. (2001)
[2] data from Gaab et al. (2005)

Table 5 Geochemistry for the samples from the Koleso valley. Main elements are given in wt%, trace element in ppm. 'bd' for below detection limit.

	Felsic Gneisses			Amphibolites			Gabbro
	02GA01	02GA06	02GA10	02GA04	02GA11	02GA12	02GA08
SiO_2	73.67	58.97	61.33	46.37	49.47	48.26	42.51
Al_2O_3	11.9	21.9	19.73	13.4	18.43	16.64	9.75
Fe_2O_3(t)	4.24	8.43	7.56	18.09	15.12	13.85	12.07
MnO	0.03	0.14	0.11	0.29	0.19	0.29	0.18
MgO	1.24	2.38	2.29	8.33	3.58	5.04	22.47
CaO	0.87	0.38	0.26	9.06	6.23	10.17	6.4
Na_2O	2.32	1.34	0.84	1.51	1.28	0.75	0.76
K2O	2.96	3.72	4.98	0.13	1.93	0.77	0.15
TiO_2	0.77	0.96	1.03	3.68	1.75	1.52	0.6
P_2O_5	0.07	0.08	0.06	0.38	0.31	0.33	0.04
Sum	98.89	99.69	99.41	101	98.96	99.23	99.79
Sc	13	13	14	42	39	42	27
V	76	113	104	512	165	285	144
Cr	57	95	84	22	798	884	1212
Co	63	44	37	98	93	98	88
Ni	29	46	45	37	206	326	354
Cu	3	20	10	37	40	29	36
Zn	63	147	129	146	92	128	78
Ga	17	31	30	28	23	21	11
Rb	101	69	206	3	74	24	8
Sr	224	161	156	387	202	377	67
Y	25	26	36	45	30	27	15
Zr	283	165	277	218	110	95	58
Nb	16	22	20	28	22	15	3
Ba	703	784	1281	bd	763	92	38
Pb	15	30	43	5	16	10	4
Th	15	16	19	bd	bd	bd	bd
U	2.6	4	2.3	bd	bd	0.9	bd
La	41	38	49	19	8	7	3
Ce	74	80	97	53	18	25	9
Pr	5	9	13	11	4	7	bd
Nd	28	34	42	30	10	7	3
Sm	4	7	9	8	1	6	2

U–Pb zircon age reflects a magmatic or a metamorphic event as the zircons reflect strong resorption and recrystallization effects. The sample itself is strongly deformed and recrystallized in amphibolite facies conditions, thus implying that metamorphism may have had great influences the U–Pb systematics of the zircons. Previously published data by Putiš et al. (2001) is, as can be seen in Fig. 4, in good accordance with the single and multigrain data of this study, if the data are reinterpreted. Putiš et al. (2001) calculated one discordia line from three of four multi-grain data points and interpreted a Variscan metamorphic event at 348 ± 31 Ma and a Cambrian magmatic event at 514 ± 24 Ma. The complete dataset can also be interpreted using two distinct discordia lines and all measured data points. According to this interpretation, the discordia (for the abraded and the HF leached fraction) reveals Precambrian ages of 1300 Ma, similar to the few old grains observed by the single grain data presented in this study, and a lower intercept at 464+9–23 Ma. The second discordia for the sieve fractions >80 µm and >60 µm reveals a similar upper intercept with a large error and a lower intercept at 330 ± 120 Ma, which may corresponds to the Variscan event (see Table 4). This new interpretation is in accordance with the pre-treatment of the multigrain fractions, because abrading and leaching removes mainly the outer parts of the zircons and old cores gain a greater influence on the ages. Therefore two main phases are recorded in the zircons of the basement in the Northern Veporic Unit: a mainly magmatic Ordovician event and a combined metamorphic-magmatic Carboniferous event. An Cretaceous metamorphic event is only locally recorded in the zircons, especially in the southern parts of the Veporic Unit (Muráň gneiss; Gaab et al., 2005).

7. Geochemistry (Koleso Valley and Kralova Hola)

Geochemical and isotope geochemical analyses were performed on samples from the Koleso Valley (Fig. 1). The results for the main and trace elements are given in Table 5. The isotopic data is given in Table 6 for the WR-Pb–Pb analyses and in Table 7 for the Sr and Nd isotopic composition.

7.1. Main and Trace Elements

Samples are classified either as felsic gneisses or as amphibolites (see Table 5). The SiO_2 content of the samples from the Koleso valley vary from 74 to 46 wt%. The total alkali contents for the felsic gneisses are between 5 and 6 wt%, whereas for the amphibolites between 1.4 and 3.2 wt%. No consistent predominance of K_2O vs. Na_2O can be observed for both lithologies. The felsic gneisses are enriched in Pb, U and REE. The amphibolites are enriched in Al_2O_3, CaO, TiO_2 and Sr.

The gabbro shows a completely different geochemistry than the amphibolites. The gabbro has very high MgO concentrations of 22.5 wt% and relatively low Fe_2O_3 concentrations of 9.75 wt%. Also Cr and Ni are quite enriched with 1212 and 354 ppm, respectively. In comparison to the amphibolites P_2O_5 and the total alkali content is significantly lower. Therefore this gabbro reflects a complete different origin, being more primitive than the amphibolites.

7.2. Whole–rock Pb isotopic composition

The WR-Pb–Pb (whole-rock Pb isotopic composition) analyses were performed to gain information on possible sources and the evolution of this unit. This dataset will be compared to the WR-Pb–Pb dataset available for the Southern Veporic Unit (Gaab et al., 2005). Additional these datasets enable a comparison of the Veporic unit with data from the Tatric unit published by Poller et al. (2001). Samples for the gabbro from the Koleso and the granites from Kralova Hola were also included. To clarify the main influences on the common lead dataset a principal component analysis was performed. This analysis rotates the axes of

Table 6 Whole Rock Pb–Pb data for samples from the Koleso valley and from Kralova Hola. Multiple splits were measured for each samples to observe the whole range of Pb isotopic composition.

	$\frac{^{206}Pb}{^{204}Pb}$	$2\sigma \times 10^{-4}$	$\frac{^{207}Pb}{^{204}Pb}$	$2\sigma \times 10^{-4}$	$\frac{^{208}Pb}{^{204}Pb}$	$2\sigma \times 10^{-4}$	$\frac{^{207}Pb}{^{206}Pb}$	$2\sigma \times 10^{-4}$
02GA01-1	18.6580	17	15.7051	16	39.2763	35	0.8417	0.03
02GA04-1	18.5152	56	15.6485	54	38.5485	118	0.8452	0.30
02GA06-1	18.3010	8	15.6706	6	38.5973	18	0.8563	0.01
02GA10-1	18.5306	13	15.7538	8	39.5476	28	0.8501	0.01
02GA10-2	18.9760	13	15.7262	9	40.5359	28	0.8287	0.01
03GA25-1	18.9812	14	15.7272	8	39.7666	31	0.8273	0.07
03GA25-2	18.8808	29	15.7148	14	39.6318	60	0.8311	0.12
03GA25-3	18.8026	8	15.6905	6	39.4111	16	0.8333	0.09
03GA25-4	18.9553	5	15.6961	17	39.2308	55	0.8269	0.14
03GA25-5	19.4093	12	15.7692	13	40.0601	26	0.8113	0.17
03GA25-6	18.9757	7	15.7263	7	39.6593	15	0.8276	0.06
03GA26-2	18.5400	8	15.6764	8	39.1016	17	0.8443	0.07
03GA31-1	18.8224	9	15.7175	8	39.2826	19	0.8338	0.07
03GA31-2	19.3528	6	15.7138	5	38.7783	12	0.8108	0.04
03GA32-1	18.9742	8	15.7155	7	39.5232	18	0.8271	0.06
03GA32-2	19.0425	17	15.7467	14	39.9142	36	0.8257	0.08
03GA32-3	18.8882	10	15.7200	9	39.5146	22	0.8311	0.07
03GA32-4	19.1397	55	15.7564	44	39.8874	114	0.8220	0.07
02GA11-1	18.7406	20	15.6828	14	38.6234	41	0.8368	0.03
02GA11-2	18.7852	5	15.6878	3	38.7153	13	0.8351	0.00
02GA11-3	18.7102	78	15.6813	57	38.7295	164	0.8381	0.45
02GA12-1	18.6988	14	15.6522	6	38.5560	29	0.8371	0.01
02GA12-2	18.7168	100	15.6769	67	38.6493	204	0.8376	0.68
02GA12-3	18.7326	70	15.7363	61	38.8699	146	0.8400	0.44
02GA08-1	18.9546	94	15.6327	67	38.3038	189	0.8247	0.64
02GA08-2	19.1008	59	15.6239	60	38.3501	119	0.8180	0.36
02GA14	19.2951	10	15.7054	9	38.7790	21	0.8140	0.01
02GA17	18.8792	10	15.7378	7	39.1364	21	0.8336	0.01

the three-dimensional Pb isotopic space that the principal components are parallel to the largest and the smallest variance of the dataset. These principal components can be interpreted as the main influences responsible for variations of the Pb data, quantifies these influences and enhances the graphical display of such datasets. The diagrams and the principal component analysis were performed using the computer script CLEO for Octave presented by Gaab et al. (2006).

The Pb isotopic compositions of the felsic gneisses in the Koleso valley are given in Table 6. The $^{206}Pb/^{204}Pb$ ratios range between 18.5 and 19.5, the $^{207}Pb/^{204}Pb$ ratios between 15.64 and 15.77 (Fig. 5). The array of these samples plot nearly along the Upper Crustal evolution line (Zartman and Haines, 1988). No age information can be retrieved from the $^{207}Pb/^{204}Pb$ vs. $^{206}Pb/^{204}Pb$ diagram for these samples, because of the large scatter. This indicates that multiple components were incorporated during formation of these gneisses.

The $^{208}Pb/^{204}Pb$ ratios vary between 38.5 and 40.7 for the Koleso gneisses. The Kralova Hola samples plot within the range of the felsic gneisses at high $^{207}Pb/^{204}Pb$ ratios between 15.62 and 15.64 and intermediate $^{208}Pb/^{204}Pb$ ratios between 38.78 and 39.14 in Fig. 5. The gabbro plots distinct from the other samples at intermediate $^{206}Pb/^{204}Pb$ and low $^{207}Pb/^{204}Pb$ and low $^{208}Pb/^{204}Pb$. This indicates a more primitive source for this gabbro with a lower Th/U ratio compared to the other samples.

Compared to the WR–Pb–Pb data published by Poller et al. (2001), the data for the Koleso gneisses fall mostly within the range of values observed for the Tatric Unit in the $^{207}Pb/^{204}Pb$ vs. $^{206}Pb/^{204}Pb$ and the $^{208}Pb/^{204}Pb$ vs. $^{206}Pb/^{204}Pb$ diagram (Fig. 5). They display relative radiogenic values and few samples plot at more radiogenic values outside the field for the Tatric unit. The samples from Kralova Hola fall in the same array at relatively high $^{207}Pb/^{204}Pb$ ratios, whereas the gabbro plots outside this array at low $^{207}Pb/^{204}Pb$ ratios.

In comparison to the Muráň gneiss, the Koleso felsic gneisses plot at more radiogenic values in the $^{207}Pb/^{204}Pb$ vs. $^{206}Pb/^{204}Pb$ as well as in the $^{208}Pb/^{204}Pb$ vs. $^{206}Pb/^{204}Pb$ diagram. The slope of a reference line would be larger for the Koleso samples than for the Muráň samples. Nevertheless, the two datasets point to a similar unradiogenic component. With a principal component analysis (Fig. 6) the differences between the datasets for the Koleso gneisses and for the Muráň gneisses can be shown: The principal component 1 observes the largest variance of 76% for the Koleso and the Muráň data set (Fig. 6A). The $^{206}Pb/^{204}Pb$, $^{207}Pb/^{204}Pb$ and the $^{208}Pb/^{204}Pb$ ratios have nearly the same influence on this main principal component. The range of the Muráň samples overlap the range of the Koleso samples. This principal component is interpreted to display mostly the radiogenic growth of Pb from U and Th. The Muráň dataset plots nearly parallel to this principal com-

Table 7 Sr and Nd isotopic data for felsic gneisses (02GA01, 02GA06, 02GA10), amphibolites (02GA04, 02GA11, 02GA12) and a gabbro (02GA08) from the Koleso area and the meta-granites from Kralova Hola (02GA14, 02GA17).

Sample	$^{87}Sr/^{86}Sr\ ^{1}_{tod}$	±2σ	$^{87}Rb/^{86}Sr$	$^{87}Sr/^{86}Sr_{ini}$	$^{143}Nd/^{144}Nd\ ^{1}_{tod}$	±2σ	$^{147}Sm/^{144}Nd$	$\varepsilon_{Nd,tod}$	$\varepsilon_{Nd,ini}$	$T\ ^{Nd}_{DM}[Ga]^4$
Koleso valley samples										
02GA01[6]	0.720803	16	1.27[2]	0.712401	0.511881	13	0.097[2]	–15	–8.9	1.8[5]
02GA06[6]	0.721154	16	1.21[2]	0.713151	0.511912	25	0.13[2]	–14	–10	1.9[5]
02GA10[6]	0.738932	92	3.73[2]	0.714286	0.511921	12	0.14[2]	–14	–10	2.0[5]
02GA04[6]	0.708375	23	0.02[2]	0.708230	0.512782	09	0.17[2]	2.8	4.5	1.1
02GA11[6]	0.715292	25	1.03[2]	0.708458	0.512519	99	0.063[2]	–2.3	5.5	0.62
02GA12[6]	0.711133	44	0.18[2]	0.709944	0.512856	10	0.19[2]	4.3	4.7	1.5
02GA08[6]	0.704393	10	0.34[2]	0.702813	0.512920	16	0.19[2]	5.5	5.9	1.2
Kralova Hola samples										
02GA14[7]	0.707460	17	0.93[3]	0.703785	0.512400	12	0.0983	–4.6	–0.5	0.94
02GA17[7]	0.711901	15	1.55[3]	0.705759	0.512398	06	0.123	–4.7	–1.7	1.2

[1] measured on TIMS *MAT261* multicollection. Errors are given as 2σ deviation of the weighted mean (6–25 blocks)
[2] calculated from the RFA merasurement (Table 5)
[3] measured on single collector ICP–MS *Element2*
[4] calculated using the depleted mantle model after Liew and Hofmann (1988)
[5] two step model at 460 Ma ($^{147}Sm/^{144}Nd = 0.12$) according Liew and Hofmann (1988)
[6] initial values calculated for 460 Ma
[7] initial values calculated for 330 Ma

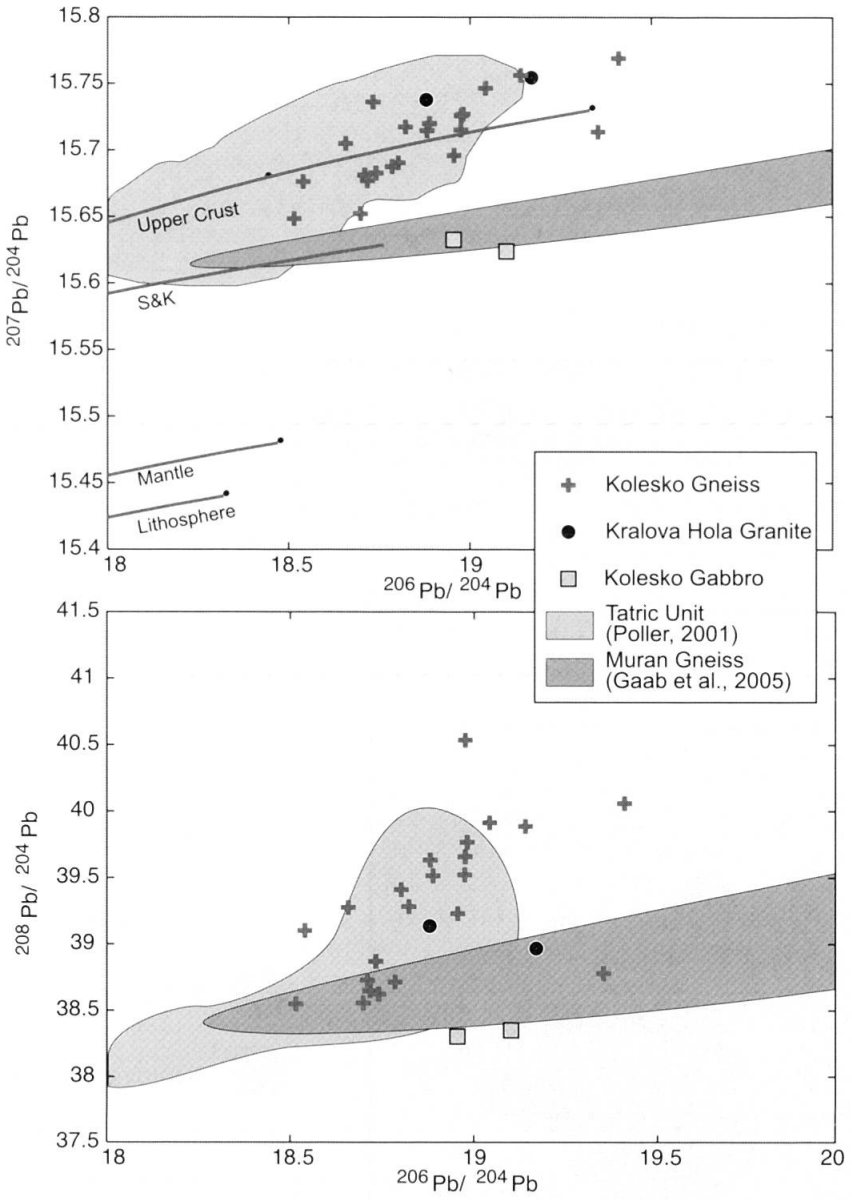

Fig. 5 $^{206}Pb/^{204}Pb$ vs. $^{207}Pb/^{204}Pb$ and $^{206}Pb/^{204}Pb$ vs. $^{208}Pb/^{204}Pb$ diagrams for the samples presented in Table 6. Evolution lines in the upper diagram drawn for the reservoirs after Zindler and Hart (1986) and the model after Stacey and Kramers (S&K; 1975).

ponent. This corresponds to the interpretation of Gaab et al. (2005) that the dataset displays the metamorphic Pb equilibration around 134 Ma reflecting the Alpine overprint.

The principal component 2 with 18.4% variance displays only a minor overlap of the two datasets. The $^{206}Pb/^{204}Pb$ correlates positively with this principle component, whereas the $^{207}Pb/^{204}Pb$ and $^{208}Pb/^{204}Pb$ are negatively correlated. In the plot of the two principal components with the largest variance, two different trends can be observed for the Muráň and the Koleso samples (Fig. 6A). This reflects a distinct evolution for both units. Nevertheless, both units have an overlap at unradiogenic values. This indicates a common source for both units. For the samples from Koleso this trend is interpreted to reflect a mixing with a radiogenic component.

The principal component 3 with 5.6% variance is plotted against the principal component 2 in Fig. 6B. The Kralova Hola granites plot distinct from the Koleso samples showing that the Kralova Hola samples do not represent the radiogenic component responsible for the variations of the Koleso samples. The gabbro in the Koleso valley plot completely distinct from the other samples in Fig. 6, thus reflecting a distinct source. The Pb isotopic variation of the Koleso samples can be interpreted as a mixing between a less evolved reservoir and more evolved crustal reservoir. The timing of this mixing can not be inferred from this dataset. The less evolved lead reservoir is compa-

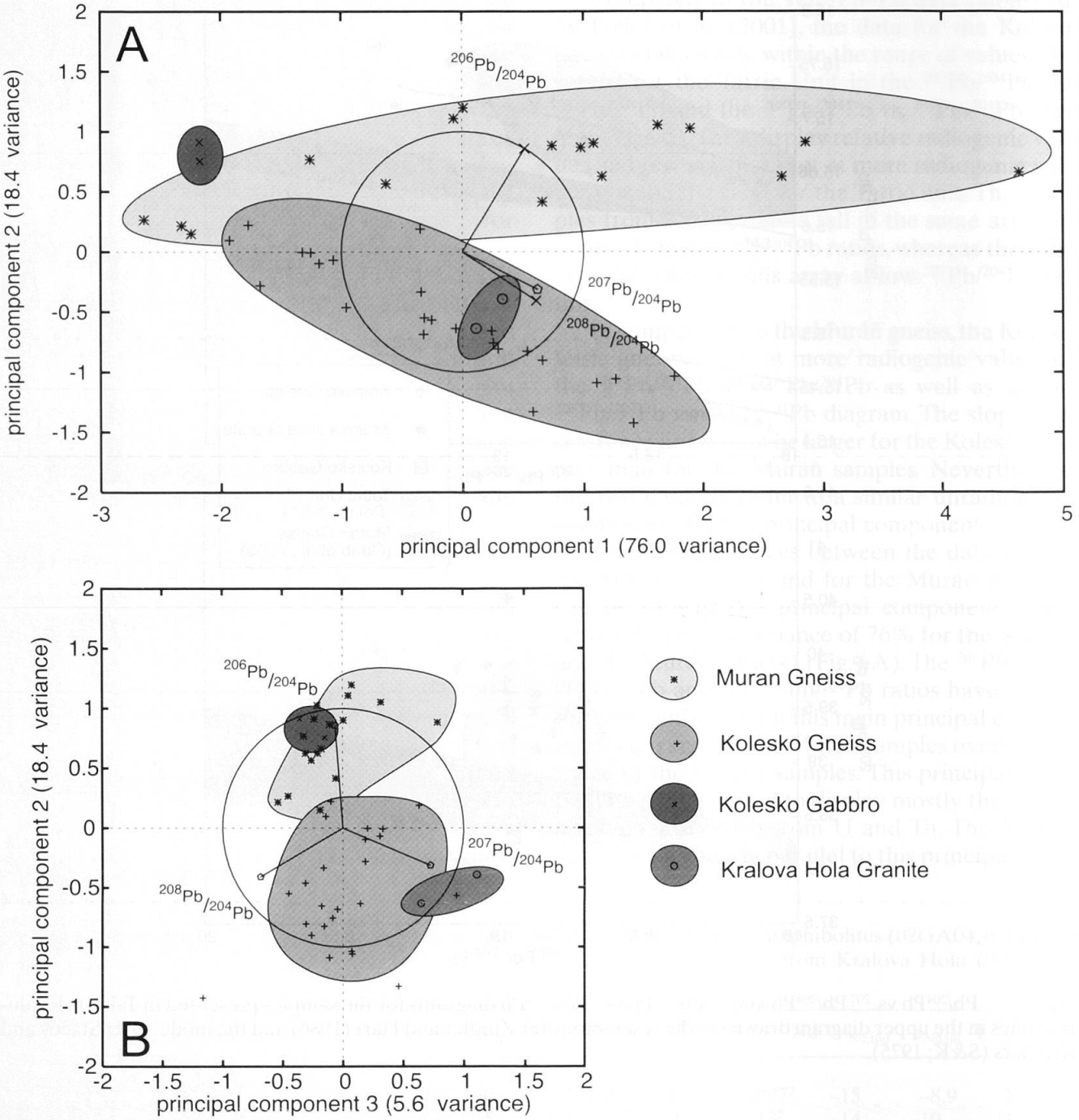

Fig. 6 Principal component analyses of the common lead data presented in this study (Table 6) together with the common lead data published in Gaab et al. (2005).

rable with the unradiogenic samples observed in the Muráň area, therefore a similar geodynamic setting for both units is inferred. The evolved crustal reservoir is characterized by high $^{207}Pb/^{204}Pb$ and $^{208}Pb/^{204}Pb$ ratios as identified by the principal component 2. This radiogenic component is not observed in the Muráň area. The Kralova Hola samples also are influenced by a crustal component. But this crustal component is distinct from the crustal component observed in the Koleso samples (Fig. 6), revealing a distinct history for these units.

7.3. Sr and Nd Isotopes

The available $^{87}Sr/^{86}Sr$ and εNd data for rocks from the Central Western Carpathians are presented in Fig. 7 to reveal different sources in these samples. The data are compared to published data on the Muráň gneiss (Gaab et al., 2005) and to the Tatric unit (Poller et al., 2001, 2005). In this diagram, the isotopic compositions are calculated back in time according to Ordovician or Carboniferous formation age. In order not to overinterprete the datasets and to include additional uncer-

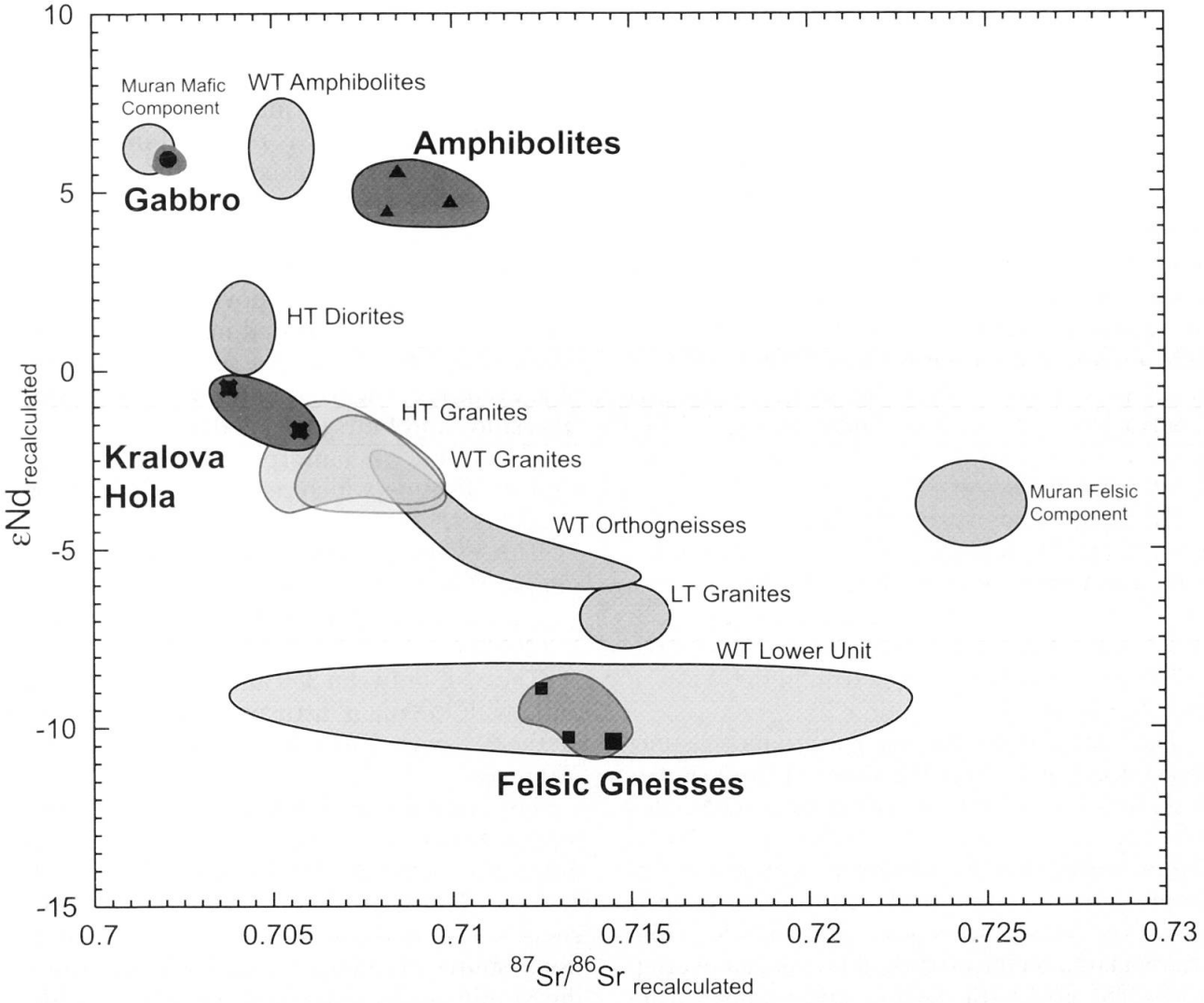

Fig. 7 εNd vs. $^{87}Sr/^{86}Sr$ diagram. Isotopic compositions are calculated back to initial values. Data for the High Tatra (HT), Western Tatra (WT), Low Tatra (LT) (Poller et al., 2001, 2005) and the Kralova Hola samples are calculated to 330 Ma, data from the Koleso valley and the Muráň area (Gaab et al., 2005) are calculated to 460 Ma.

tainties of the exact formation age, the samples are either recalculated to initial values at 460 Ma or at 330 Ma, respectively. The data for the Tatra mountains from Poller et al. (2001, 2005) are recalculated to 330 Ma, except the data for the metasediments from the Lower Unit in the Western Tatra Mountains, which are recalculated to 460 Ma. The samples presented in this study are recalculated to 460 Ma, except the Kralova Hola samples, which formed during the Variscan orogeny (see Fig. 4). The data of the Muráň area are plotted according to the interpretation presented in Gaab et al.(2005).

Two distinct groups can be recognized in Fig 7. The amphibolites form a small array at radiogenic $^{87}Sr/^{86}Sr_{ini,460}$ values of 0.710 to 0.708 with radiogenic $\varepsilon Nd_{ini,460}$ values between 4 and 6. This array does not coincide with the primitive mantle composition of Zindler and Hart (1986), thus indicating either a crustal contamination or a non-primitive source composition. All felsic samples plot in a narrow array between 0.712 to 0.715 and –10 to 8 for $^{87}Sr/^{86}Sr_{ini,460}$ and $\varepsilon Nd_{ini,460}$, respectively. These values reflect a major influence of an evolved crustal component in these samples.

The gabbro sample from the Koleso area plots at low $^{87}Sr/^{86}Sr_{ini,460}$ values of 0.703 and $\varepsilon Nd_{ini,460}$ values of 6, reflecting a more primitive source as the amphibolites. Initial values for this sample are calculated at 460 Ma.

The Kralova Hola samples vary between 0.703 to 0.706 for $^{87}Sr/^{86}Sr_{ini,330}$ and –1.7 to –0.5 for $\varepsilon Nd_{ini,330}$, which are values close to the bulk earth composition after Zindler and Hart (1986). The mylonitized sample plots at slightly higher εNd_{ini} and lower $^{87}Sr/^{86}Sr_{ini}$, which is probably due to a slight redistribution of the parent-daughter ratios during deformation and metamorphism. Neverthe-

less are the initial values comparative with the undeformed sample. The mean crustal resident ages, $T^{Nd}/_{DM}$ for the samples are presented in Table 7.

Two age groups become evident. The felsic samples result in old $T^{Nd}/_{DM}$ between 2.0 and 1.8 Ga using a two step approach with 460 Ma as age for the second step. These results fit well with $T^{Nd}/_{DM}$ for the Lower Unit in the Western Tatra between 2.0 and 1.8 Ga (Poller et al., 2001). All mafic sample reveal younger $T^{Nd}/_{DM}$ between 1.5 and 0.6 Ga and thus have crustal resident ages comparable to common granitic rocks from the Tatric unit (Kohút et al., 1999; Poller et al., 2001). The Kralova Hola granite has similar young $T^{Nd}/_{DM}$ between 1.2 and 1 Ga, the gabbro in the Koleso Valley has a $T^{Nd}/_{DM}$ of 1.2 Ga.

In comparison with published data for the Western and High Tatra Mountains (Poller et al., 2001), the basement rocks from the Koleso area can be clearly distinguished. The felsic gneisses have lower εNd and are only comparable with the meta sediments of the Lower Unit in the Western Tatra Mountains.

The amphibolites and the gabbro plot distinct from amphibolites from the Western Tatra (Poller et al., 2005) and from the other reference fields from the Tatra Mountains (Poller et al., 2001). This indicates, that the Veporic basement has different sources as the Tatric unit which formed during the Variscan orogeny. The samples from Kralova Hola on the other hand reveal an overlap in $^{87}Sr/^{86}Sr$ εNd with diorites and granites from the High Tatra Mountains (Poller et al., 2001). Thus the Kralova Hola is not only similar in age with the Tatric unit, but also in the isotopic composition. The Muráň gneiss felsic component presented in Gaab et al. (2005) in the Southern Veporic Unit plot distinct from the Koleso samples. The felsic member has too high $^{87}Sr/^{86}Sr$ ratios and too high εNd values compared to the felsic gneisses. The Muráň mafic component coincides with the gabbro from the Koleso valley, but not with the amphibolites (Fig. 7).

8. Conclusion

A common evolution for the whole Veporic Unit in Paleozoic times is suggested from the U–Pb zircon data presented in this study. The apparent dichotomy, which arises with comparison of literature data (Putiš et al., 2001), can be circumvented, if the literature data are reinterpreted. Still more data are needed, especially in the Southern Veporic Unit, to really ensure this common evolution for all basement units in the Veporic Unit. At least three major events can been recognized in the geochronologic U–Pb data from the Northern Veporic Unit:

(1) Major Ordovician magmatic event (470–460 Ma), followed by minor magmatic activity (≈ 440 Ma). This event is recorded in all samples presented in this study except in the granites from Kralova Hola.

(2) Variscan magmatic and metamorphic event (350–330 Ma) with formation of granitoids and recrystallization of Ordovician basement. The magmatic event is recorded in the Kralova Hola granites and the Drotacka sample. A metamorphic event is recognized in the Hoškova samples (this study and Putiš et al., 2001).

(3) Alpine metamorphic event during the Cretaceous time, which caused locally lead loss in the zircons.

This event is mainly recorded in the Muráň sample (Gaab et al., 2005), according to the increasing metamorphic grade observed by Janák et al. (2001a).

The ages between 350 and 340 Ma are comparable with the main intrusive activity for granites in the Western Tatra Mountains (Poller et al., 2000).

The common lead data together with the isotopic data from the Koleso valley reveal a marked difference between the Northern Veporic Unit and the Southern Veporic Unit (i.e. the Muráň gneiss). It reveals an important role of an additional source of radiogenic lead, which is absent in the Muráň gneiss. This source could not be identified within the Veporic unit, but is characterized by high $^{207}Pb/^{204}Pb$ and $^{208}Pb/^{204}Pb$ ratios and therefore represents a typical crustal source. The Kralova Hola granites point in a similar direction as this source, but do not coincide exactly with the observed variations as demonstrated by the principal component analysis.

The εNd and the $^{87}Sr/^{86}Sr$ isotopic compositions of the felsic gneisses in the Northern Veporic Unit are similar to the metasedimentary Lower Unit in the Western Tatra and distinct from the other units observed in the Tatra Mountains and in the Veporic unit. The Lower Unit has a minimum sedimentation age of ≈ 500 Ma according to U–Pb zircon studies (Gurk, 1999; Gurk and Poller, 1999) and therefore can not be attributed as sediments derived from these rocks.

The amphibolites in the Koleso valley, which were metamorphosed under HP metamorphic conditions (Janák et al., 2003), are distinct in their εNd and $^{87}Sr/^{86}Sr$ isotopic composition from the amphibolites from the Western Tatra Mountains (Poller et al., 2005). They are characterized by relatively high $^{87}Sr/^{86}Sr_{ini}$ and slightly lower εNd thus reflecting a distinct source. They are also dis-

tinct in their εNd and $^{87}Sr/^{86}Sr$ composition from the Muráň mafic member observed in the Southern Veporic Unit (Gaab et al., 2005). Only the gabbro from the Koleso valley depicts marked similarities with the Muráň mafic component, suggesting common sources.

Acknowledgements

J. Huth is thanked for help at the electron microscope for cathodo-luminescence imaging. D. Neuhäuser for her help and presence at the clean-lab. A. Hofmann is gratefully acknowledged for providing the opportunity to perform this study at MPI, Mainz. The field work has been partly supported (to Janák) from grants APVT-20-020002 and VEGA 3167. Helpful reviews by Prof. U. Schaltegger, Dr. habil. M. Tichimirowa and Dr. J.-L. Paquette are greatly acknowledged.

References

Andrusov, D. (1958): Geology of Czechoslovak Carpathians I (In Slovak with Russian and German summary). SAV Publisher, Bratislava.

Cambel, B., Král', J. and Burchart, J. (1990): Izotopová geochronológia kryštalinka západných karpát. VEDA.

Compston, W., Williams, I. and Meyer, C. (1984): U–Pb geochronology of zircons from lunar breccia 73217 using a sensitive high mass-resolution ion microprobe. *J. Geoph. Res.* **89**, B525–B534. Supplement.

Dallmeyer, R.D., Neubauer, F., Handler, R., Fritz, H., Müller, W., Pana, D. and Putiš, M. (1996): Tectonothermal evolution of the internal Alps and Carpathians: Evidence from $^{40}Ar/^{39}Ar$ mineral and whole-rock data. *Eclogae geol. Helv.* **89**, 203–227.

Finger, F., Broska, I., Haunschmid, B., Hraško, L., Kohút, M., Krenn, E., Petrík, I., Riegler, G. and Uher, P. (2003): Electron-microprobe dating of monazites from Western Carpathian basement granitoids: plutonic evidence for an important Permian rifting event subsequent to Variscan crustal anatexis. *Int. J. Earth Sci.* **92**, 86–98.

Gaab, A., Janák, M., Poller, U. and Todt, W. (2005): Alpine reworking of Ordovician protoliths in the Western Carpathians: Geochronological and geochemical data on the Muráň Gneiss Complex. *Lithos* **87**, 261–274.

Gaab, A., Todt, W. and Poller, U. (2006): CLEO: Common lead evaluation using Octave. *Computers & Geosciences* **32**, 993–1003.

Gurk, C. (1999): Petrographie, Geochemie und Geochronologie der unteren Einheit, Tatricum, Westliche Tatra (Slovakei). Unpublished Diploma Thesis, University of Mainz.

Gurk, C. and Poller, U. (1999): Petrography, geochemistry and geochronology of the Lower Unit, Western Tatra Mts (Slovakia). EUG Journal of Conference Abstracts 4, p. 809.

Janák, M., Cosca, M., Finger, F., Plašienka, D., Koroknai, B., Lupták, B. and Horváth, P. (2001a): Alpine (Cretaceous) metamorphism in the Western Carpathians: P-T-t paths and exhumation of the Veporic core complex. *Geologisch-Paläontologische Mitteilungen Innsbruck* **25**, 115–118.

Janák, M., Finger, F., Plašienka, D., Petrík, I., Humer, B., Méres, Š. and Lupták, B. (2002): Variscan high P–T recrystallization of Ordovician granitoids in the Veporic unit (Nízke Tatry Mountains, Western Carpathians): new petrological and geochronological data. *Geolines* **14**, 38–39.

Janák, M., Méres, Š. and Ivan, P. (2003): First evidence for omphacite and eclogite facies metamorphism in the veporic unit of the Western Carpathians. *Journal of the Czech Geological Society* **48**, 69.

Janák, M., Plašienka, D., Frey, M., Cosca, M., Schmidt, S., Lupták, B. and Méres, Š. (2001b): Cretaceous evolution of a metamorphic core complex, the Veporic unit, Western Carpathians (Sovakia): P–T conditions and in situ $^{40}Ar/^{39}Ar$ UV laser probe dating of metapelites. *J. Metamorphic Geol.* **19**, 197–216.

Klinec, A. (1966): Zum Bau und Bildung des Veporiden-Kristallin. *Sbor. Geol. vied, Západné Karpaty* (In Slovak with German Summary).

Kohút, M., Kovach, V.P., Kotov, A.B., Salinkova, E.B. and Savatenkov, V.M. (1999): Sr and Nd isotope geochemistry of hercynian granitic rocks from the Western Carpathians – Implications for granite genesis and crustal evolution. *Geologický Zbornik - Geologica Carpathica* **50**, 477–487.

Koroknai, B., Horvath, P., Balogh, I.K. and Dunkl, I. (2001): Alpine metamorphic evolution and cooling history of the Veporic basement in northern Hungary: new petrological and geochronological constraints. *Int. J. Earth Sci.* **90**, 740–751.

Kováčik, M., Král', J. and Maluski, H. (1996): Metamorphic rocks in the Southern Veporicum basement: their Alpine metamorphism and thermochronologic evolution. *Mineralia Slovaca* **28**, 185–202.

Král', J., Frank, W. and Bezák, V. (1996): $^{40}Ar–^{39}Ar$ spectra from amphibole of veporic amphibolic rocks. *Mineralia Slovaca* **28**, 501–513.

Liew, T. and Hofmann, A. (1988): Precambrian crustal components, plutonic associations, plate environment of Hercynian Fold Belt of central Europe: Indications from a Nd and Sr isotopic study. *Contrib. Mineral. Petrol.* **98**, 129–138.

Ludwig, K.R. (2001a): Isoplot/ex rev. 3.49 A geochronological Toolkit for Microsoft Excel. *Berkeley Geochronological Center; Special Publications* No. **1a** .

Ludwig, K.R. (2001b): SQUID 1.02 – A user's Manual. *Berkeley Geochronological Center; Special Publications* No. **2**.

Lupták, B., Janák, M., Plašienka, D., Schmidt, S.T. and Frey, M. (2000): Chloritoid-kyanite schists from the Veporic unit, Western Carpathians, Slovakia: implications for Alpine (Cretaceous) metamorphism. *Schweiz. Mineral. Petrogr. Mitt.* **80**, 211–222.

Lupták, B., Janák, M., Plašienka, D. and Schmidt, S.T. (2003): Alpine lowgrade metamorphism of the Permian–Triassic sedimentary rocks from the Veporic Superunit, Western Carpathians: Phyllosilicate composition and "crystallinity" data. *Geologický Zbornik - Geologica Carpathica* **54**, 367–375.

Lupták, B., Thöni, M., Janák, M. and Petrík, I. (2004): Sm–Nd isotopic chronometry of garnets from the veporic unit, Western Carpathians: some preliminary age results and P–T constraints. *Geolines* **17**, p. 66.

Maluski, H., Rajlich, P. and Matte, P. (1993): $^{40}Ar/^{39}Ar$ dating of the Inner Carpathians Variscan basement and Alpine mylonitic overprinting. *Tectonophysics* **223**, 313–337.

Plašienka, D., Grecula, P., Putiš, M., Hovorka, D. and Kovac, M. (1997): Evolution and structure of the Western Carpathians: an overview. In: Grecula, P., Hovorka, D., Putiš, M. (Eds.), Geological Evolution of the Western Carpathians. *Mineralia Slovaca - Monograph*, 1–24.

Poller, U., Janák, M., Kohút, M. and Todt, W. (2000): Early Variscan Magmatism in the Western Carpathians: U–Pb zircon data from granitoids and orthogneisses

of the Tatra Mts (Slovakia). *Int. J. Earth Sci.* **89**, 336–349.

Poller, U., Kohút, M., Gaab, A. and Todt, W. (2005): Pb, Sr and Nd isotope study of two co-existing magmas in the Nízke Tatry Mountains, Western Carpathians (Slovakia). *Mineralogy and Petrology* **84**, 215–231.

Poller, U., Kohút, M., Todt, W. and Janák, M. (2001): Nd, Sr, Pb isotope study of the Western Carpathians: implications for Palaeozoic evolution. *Schweiz. Mineral. Petrogr. Mitt.* **81**, 159–174.

Poller, U. and Todt, W. (2000): U–Pb single zircon data of granites from the High Tatra Mountains (Slovakia): implications for the geodynamic evolution. *Trans. R. Soc.* **91**, 235–243.

Poller, U., Uher, P., Broska, I., Plašienka, D. and Janák, M. (2002): First Permian–Early Triassic zircon ages for tin-bearing granites from the Gemeric unit (Western Carpathians, Slovakia): connection to the post-collisional extension of the Variscan orogen and S-type magmatism. *Terra Nova* **14**, 41–48.

Putiš, M., Filová, I., Korikovsky, S.P., Kotov, A.B. and Madarás, J. (1997): Layered metaigneous complex of the veporic basement with features of the Variscan and Alpine thrust tectonics (Western Carpathians). In: Grecula, P., Hovorka, D. and Putiš, M. (Eds.), Geological Evolution of the Western Carpathians. *Mineralia Slovaka - Monograph, Geocomplex*, 175–196.

Putiš, M., Kotov, A., Korikovsky, S., Salnikova, E., Yakoleva, S., Berezhnaya, N., Kovach, V. and Plotkina, J. (2001): U–Pb zircon ages of dioritic and trondhjemitic rocks from a layered amphibolitic complex crosscut by granite vein (Veporic basement, Western Carpathians). *Geologický Zbornik - Geologica Carpathica* **52**, 49–60.

Stacey, J.S. and Kramers, J.D. (1975): Approximation of terrestrial lead isotope evolution by a two-stage model. *Earth Planet. Sci. Lett.* **26**, 207–221.

Thöni, M., Petrík, I., Janák, M. and Lupták, B. (2003): Preservation of Variscan garnet in Alpine metamorphosed pegmatite from the Veporic unit, Western Carpathians: evidence from Sm–Nd isotope data. *Journal of the Czech Geological Society* **48**, 123–123.

Todt, W., Cliff, R., Hanser, A. and Hofmann, A. (1996): Earth Processes: Reading the Isotopic Code, chapter: $^{202}Pb + {}^{205}Pb$ double spike for lead isotopic analyses. *Geophysical Monograph*, vol. **95**, 429–437.

Vozárová, A., Sotáck, J. and Ivanička, J. (1998): A new microfauna from the Early Paleozoic fromations of the Gemericum (foraminifera): constraints for another fossils or subfossils. In: Rakús, M. (Ed.), Geodynamic development of the Western Carpathians. Dionýz Stúr Publication, 47–61.

Wendt, J. and Todt, W. (1991): A vapor digestion method for dating single zircons by direct measurement of U and Pb without chemical separation. *Terra Abstracts* **3**, 507–508.

White, W. and Patchett, J. (1984): Hf–Nd–Sr isotopic and incompatible element abundances in island arcs: implications for magma origins and crust-mantle evolution. *Earth Planet. Sci. Lett.* **67**, 167–185.

Williams, I. (1998): U–Th–Pb Geochronology by Ion-Microprobe. In: McKibben, M., Shanks III, W., Ridley, W. (Eds.), Application of microanalytical techniques to understanding mineralization processes, vol. **7** of *Reviews in Economic Geology*. The Society of Economic Geologists, 1–35.

Zartman, R. and Haines, S. (1988): The plumbotectonic model for Pb isotopic systematics among major terrestrial reservoirs – A case for bi-directional transport. *Geochim. Cosmochim. Acta* **52**, 1327–1339.

Zindler, A. and Hart, S. (1986): Chemical Geodynamics. *Annual Review of Earth and Planetary Sciences* **14**, 493–571.

Zoubek, V. (1957): Grenze Zwischen den Gemeriden und Veporiden (In Slovak with German Summary). *Geol. Prace*, Zoit **46**, 38–50.

Received 22 April 2005
Accepted in revised form 9 September 2005
Editorial handling: U. Schaltegger